Cold versus hot shear banding in bulk metallic glass

Y. Q. Cheng,[1] Z. Han,[2] Y. Li,[2,*] and E. Ma[1,†]
[1]*Department of Materials Science and Engineering, Johns Hopkins University, Baltimore, Maryland 21218, USA*
[2]*Department of Materials Science and Engineering, National University of Singapore, Singapore 117576, Singapore*
(Received 31 August 2009; published 19 October 2009)

We present an analysis of the shear-banding dynamics in a bulk metallic glass (BMG), including the temperature rise in the band, the sliding speed of the band, and the time elapsed as well as the step size of the shear offset growth in a stop-and-go cycle. This model analysis quantitatively demonstrates that the major shear band can remain cold and slide in a stick-slip manner. We predict that the shear step (distance covered by a stop-and-go cycle) scales with the sample size and machine stiffness. We also illustrate the conditions when such serrated shear is unsustainable and a hot shear band directly develops in a runaway instability (catastrophe). These findings provide physical insight into the shear-instability processes and offer useful information for improving the plasticity of BMGs. The calculation results are used to explain several intriguing recent experimental observations, including the stick slip of the dominant shear-band and the sample-size effects on the plastic-flow behavior of BMGs.

DOI: 10.1103/PhysRevB.80.134115 PACS number(s): 61.43.Dq, 62.20.F−

I. INTRODUCTION

For the emerging bulk metallic glasses (BMGs),[1] shear banding is known to be the dominant plastic-deformation mode at room temperature (T_R).[2–7] However, despite tremendous current interest, the shear bands in these amorphous metals remain poorly understood. Upon loading a BMG, one usually observes a dominant shear band. The temperature (T) reached inside the shear band is currently a subject under intense debate.[8–14] Unless blocked or diverted (e.g., by nanoscale entities such as crystals[2–7]), such a shear band could have catastrophic consequences, ending the plastic strain observable for the BMG.

However, the shear banding does not have to be always fatal. In Fig. 1, we observe a very different type of shear-band behavior. Here the stress-strain curve shows clear serrations [Fig. 1(a)] that correspond to the stop-and-go sliding of the major shear band, for a cylindrical $Zr_{64.13}Cu_{15.75}Ni_{10.12}Al_{10}$ BMG (Ref. 6) sample with diameter $d=1.0$ mm. The repeated sliding of the shear band leads to large plastic strains without catastrophic failure [Fig. 1(c)]. Similar observations have been reported before in this BMG (Refs. 15 and 16) and other related BMGs. On the sheared-apart surfaces, the stop-and-go sliding corresponds to striations with regular spacing [Fig. 1(b)] while the vein-like pattern typical for a catastrophic event[2] is not observed. In recent experiments, the striation spacing is found to scale with the sample size for $d=1.0$, 1.5, and 2.0 mm (see Table I).[17,18]

These observations raise important questions regarding the fundamental shear-banding physics in BMGs. First, under what machine/sample conditions would the dominant shear band exhibit such stick-slip serration and when would the band become an unstoppable runaway catastrophe instead?[17,19] Second, what is the mechanism that underlies the different behaviors? Third, what is the T reached inside the shear band for these two bifurcated scenarios,[10,11] especially for the controlled (or noncatastrophic) shear-banding cases? Fourth, how does the shear step/offset grow and what controls its velocity and the step size? These intriguing questions are important for understanding the plastic flow of amorphous solids.

This paper presents quantitative answers to these intriguing questions, using a model that goes beyond previous treatments[8,10,11] (see discussion in Sec. III). In particular, our

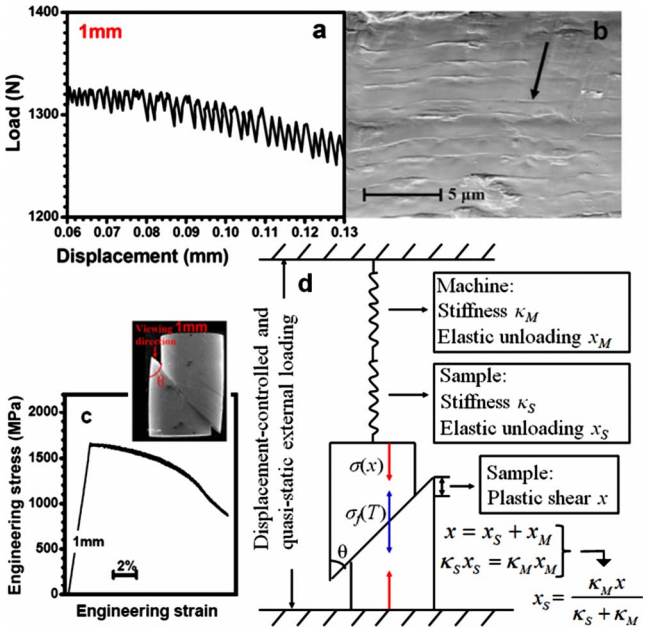

FIG. 1. (Color online) (a) Serrated load-displacement curve, (b) striations (an example is pointed to by an arrow) on the sheared-apart surface, and (c) the entire stress-strain curve (showing large plastic strains) of a sample with $d=1$ mm and an aspect ratio of 2:1. The inset in (c) shows the sample after test and the viewing direction for the micrograph in (b) (Ref. 18). (d) shows a schematic of the machine-sample system during sliding as well as the relationship between the elastic unloading of the machine and the sample and the plastic shear (the external loading is quasistatic for the short shear-band-sliding time).

TABLE I. Shear step size (Δx) and temperature rise (ΔT) for a single shear-band-slip event calculated using Eq. (6), in comparison with experimental measurements on different sample sizes (diameter d and aspect ratio 2:1) and shear-band-instability index (S) (Ref. 18).

d (mm)		1.0	1.5	2.0	3.0	4.0
S		1.34	1.79	2.20	2.99	3.91
Δx (μm)	Eq. (6)	1.51	3.56	8.41	no stop	no stop
	Expt.[a]	1.15–1.84	3–4.83	3–9	no stop	no stop
ΔT (K), Eq. (6)		2.4	5.9	13.9	$>T_g$	$>T_g$

[a]Reference 18.

analysis in the following demonstrates that the stop-and-go behavior arises from the "cold" nature of the shear band.

II. MODEL ASSUMPTIONS AND DERIVATION

To model the shear-banding process in a laboratory loading test, an exact description would be rather difficult due to many complicating factors under various experimental conditions. We will, therefore, attempt to simplify the process by capturing the controlling factors. Several assumptions, and the related justifications, are given below as we derive the model.

Similar to the case of static/kinetic friction,[20] the activation stress of an shear band (yield stress, σ_y) is expected to be higher than the quasiequilibrium stress needed for running a sliding shear band (flow stress, σ_f) at the same T.[21,22] This is due to the kinetic softening associated with the structural disordering, chemical alienation,[21] and volumetric dilatation (such as free volume generation) in the flowing material. In a sliding shear band, the instantaneous σ_f should depend on the current T and strain rate $\dot{\varepsilon}$ *within* the band (thickness $\sim$10 nm).

The local flow of the material in the thin shear band can be considered homogeneous thus the flow stress σ_f is proportional to the product of viscosity (η) and strain rate.[16] Depending on the combination of T and $\dot{\varepsilon}$, the flow can be either Newtonian (constant η) or non-Newtonian (nonconstant η).[16,23,24] In a metallic glass/liquid, low T and/or high $\dot{\varepsilon}$ leads to non-Newtonian behavior, and the typical T range ($<T_g$, the glass-transition temperature) and $\dot{\varepsilon}$ range inside the shear band [estimated to be 10^3–10^5/s (Ref. 16)] bring the shear-band material deeply into the non-Newtonian regime in the η-$\dot{\varepsilon}$ plot, where the equilibrium η drops steadily with increasing $\dot{\varepsilon}$ (i.e., shear thinning, see Refs. 16, 23, and 24 for representative η-$\dot{\varepsilon}$ plots). In such a regime, it is interesting to note that the product of η and $\dot{\varepsilon}$, i.e., σ_f, is not sensitive to $\dot{\varepsilon}$ itself (when T is fixed). This seems to be a coincidence but essentially it reflects the nature of the non-Newtonian flow in metallic glass/liquid. To further justify the above argument, we have employed computer simulations of a $Cu_{64}Zr_{36}$ metallic glass. The details of simulation can be found in Ref. 22. The result in Fig. 2(a) clearly demonstrates the insensitive strain-rate dependence of the σ_f. Note that although the simulated $\dot{\varepsilon}$ is several orders of magnitude higher than the estimated $\dot{\varepsilon}$ in a shear band, these strain rates fall on the same line in the same non-Newtonian regime in the η-$\dot{\varepsilon}$ plot. The trend in Fig. 2(a) is therefore expected to be followed.

On the other hand, σ_f is found to decrease almost linearly with increasing T in our simulation and the trend is shown in Fig. 2(b). In fact, experiments suggest that the T dependence of σ_f may follow a universal linear relation:[25]

$$\sigma_f(T) = \sigma_f(T_R + \Delta T) \approx \sigma_f - AE\Delta T/T_g, \tag{1}$$

where A is a dimensionless constant determined to be $\sim$0.0106 for various BMGs and E is the Young's modulus of

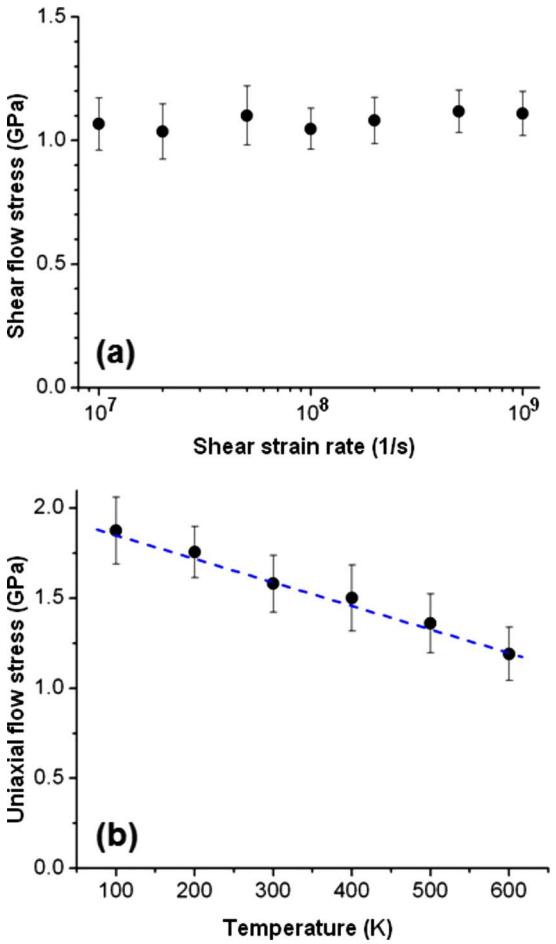

FIG. 2. (Color online) (a) Strain rate and (b) temperature dependence of flow stress in a simulated $Cu_{64}Zr_{36}$ metallic glass (see Ref. 22 for details of simulation). The temperature in (a) was fixed at 50 K. The dashed line in (b) is a linear fit of the data (see text).

the BMG.[25] In our case, ΔT is the temperature rise in the band above room temperature (T_R). It is found that Eq. (1) and the constant A are also applicable to the simulation results in Fig. 2(b); there the fit (the dashed line) matches the linear dependence predicted by Eq. (1) using $A=0.0106$ and the properties of this particular MG [$Cu_{64}Zr_{36}$, $E=92$ GPa, $T_g=787$ K (Ref. 26), and $T_R=300$ K].

Our model assumes that the machine-sample system (MSS) is subjected to displacement-controlled and quasistatic external loading. The fast shear-band sliding is then an internal event in the closed MSS. The sample is initially loaded to reach σ_y. Once the flow is activated and the shear band starts to slide, the resistance (σ_f) in the shear plane is smaller than the internal stress. The excess stress (σ_y-σ_f) causes the acceleration of, and the associated strain redistribution in, the MSS. Note that in the above model, the major shear band operates across the entire sample simultaneously after activation. In other words, although the activation of the shear band (or mobilization of atoms in the shear plane) may be accomplished by the propagation of shear waves in certain form (at a velocity close to the speed of sound), the subsequent sliding and growth of the shear offset proceed in a cooperative manner. Such a "cooperative shear" scenario (for the major shear band) is supported by experimental observations in Refs. 15–18 and 27.

During shear band sliding, the elastic energy stored in the MSS is released, involving elastic unloading of *both* the machine and the sample, as well as the plastic shear of the shear band (the sum of the displacements, defined in Fig. 1(d), is effectively zero). The governing kinetic equation, written for the vertical uniaxial loading direction, is

$$[\sigma(x) - \sigma_f(T)]\frac{\pi d^2}{4} = Mx'', \tag{2}$$

where $\sigma(x)$ is the internal stress in the MSS. $\sigma(0)=\sigma_y$, and due to the elastic unloading $\sigma(x)$ decreases with increasing sample displacement (x) that accompanies the corresponding plastic shear. $\sigma_f(T)$ is a function of the local T at the given moment in the shear band (Eq. (1)). M is the effective inertia of the MSS when responding to the stress gradient and is an empirical parameter estimated to be on the order of 10–100 kg for a typical MSS (see discussion in the next section). x'' is the second derivative of x, i.e., the acceleration. Using the parameters defined in Fig. 1(d), we have

$$\sigma(x) = \sigma_y - E\frac{x_S}{L} = \sigma_y - \frac{E}{L}\frac{\kappa_M}{(\kappa_S + \kappa_M)}x = \sigma_y - \frac{Ex}{L(1+S)}, \tag{3}$$

where L is the sample height, E is the Young's modulus, and S is defined by $S=\frac{\kappa_S}{\kappa_M}=\frac{\pi d^2 E}{4L\kappa_M}$ in Ref. 17. The elastic unloading associated with the increasing shear displacement x gradually reduces the driving stress for accelerating the slide.

At the same time, however, the resistance $\sigma_f(T)$ is also decreasing with increasing x, as T is elevated by ΔT in the shear band due to the concentrated deformation (Eq. (1)). The energy source of the T increase is the plastic work in the shear band. The plastic work is fully converted into heat when the flow reaches a quasisteady state but for the initial-structural rejuvenation, part of the plastic work is stored in the shear band as configurational potential energy.[28] This latter-structural rejuvenation, however, should be accomplished with a local strain of less than 100%.[22] For the whole sliding length of each stick-slip cycle (on the order of $\sim\mu$m, $>10\,000\%$ local strain), the energy cost for rejuvenation is a very small fraction and negligible. The heat flux (heat flow per unit area per unit time) dumped into the shear band is thus a function of time (t) and scales with sliding speed. As a first-order approximation, it can be expressed as

$$f(t) = E\varepsilon_y x' \sin\theta, \tag{4}$$

where ε_y is the yield strain, which is almost a constant (2%),[29] and θ is the shear band angle [Fig. 1(d)]. x' is the first derivative of x, i.e., instantaneous vertical-sliding speed, which is also a function of time t. The "first-order approximation" refers to the use of a constant $E\varepsilon_y$ term to represent the average stress level in the sample during sliding. The stress in fact oscillates with the serration but the amplitude is small [Fig. 1(c)].

Considering the shear band as a two-dimensional heat source with heat flux $f(t)$, and the sample body as a three-dimensional heat-conducting medium, the instantaneous T rise in the shear band is[30]

$$\Delta T(t) = \frac{1}{2\rho c_p\sqrt{\pi\alpha}}\int_0^t f(t-\tau)\frac{d\tau}{\sqrt{\tau}}, \tag{5}$$

where ρ is the (sample) mass density, c_p is the heat capacity, and α is the thermal diffusivity.

By substituting Eq. (4) into Eq. (5), and then plugging Eqs. (1), (3), and (5) into Eq. (2), the governing kinetic equation is then

$$\left[\left(\sigma_y - \frac{Ex}{L(1+S)}\right) - \left(\sigma_f - \frac{AE^2\varepsilon_y \sin\theta}{2\rho c_p T_g\sqrt{\pi\alpha}}\int_0^t x'\times(t-\tau)\frac{d\tau}{\sqrt{\tau}}\right)\right]\frac{\pi d^2}{4} = Mx'' \tag{6}$$

with boundary conditions $x(0)=0$ and $x'(0)=0$. It should be noted that the above model is only applicable at small overall sample plastic strains, when the loading geometry and the uniaxial stress state are not noticeably affected by the shear off. The later stage of the stress-strain curve in Fig. 1 (i.e., when the sample has been significantly deformed) is beyond the scope of the present discussion.

III. RESULTS AND DISCUSSION

If we were to ignore the T rise, the serration cycle could be solved analytically from Eq. (6), explicitly giving the shear step size

$$\Delta x = \frac{2(\sigma_y - \sigma_f)}{E}L(1+S). \tag{7}$$

Substituting Eq. (7) for x in Eq. (3), the corresponding stress drop when the band stops is then $2(\sigma_y$-$\sigma_f)$. Equation (7) implies that for a cold sliding shear band, there is no intrinsic

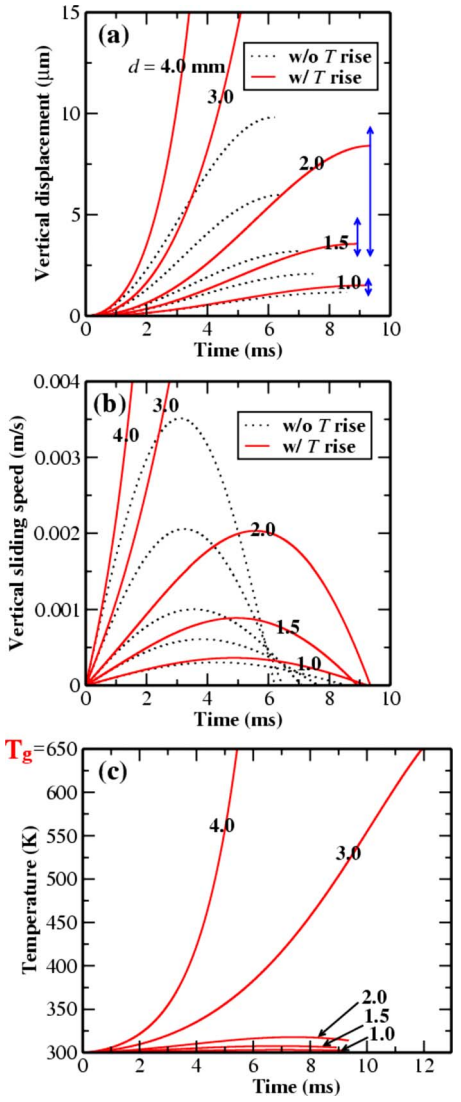

FIG. 3. (Color online) Evolution of (a) vertical displacement (x), (b) vertical sliding speed (v), and (c) temperature in the shear band (T), all as a function of shear-band-sliding time t. Solid red lines are model predictions with the T rise considered; dotted black lines are model solutions without the T effect; vertical blue bars represent the range of experimentally measured step size for corresponding samples (Table I) (Ref. 18). The material properties used are: $E=80$ GPa, $\rho=6.5\times10^3$ kg/m^3, $c_p=350$ J/(kg·K), $\alpha=2.2\times10^{-6}$ m^2/s, $T_g=650$ K, $\theta=45°$, and $T_R=300$ K for $Zr_{64.13}Cu_{15.75}Ni_{10.12}Al_{10}$ BMG (Refs. 6 and 15–18).

mechanism for catastrophe; the step size simply scales with $L(1+S)$ and the stress drop is a constant-material property.

For $Zr_{64.13}Cu_{15.75}Ni_{10.12}Al_{10}$, the observed stress drop in Fig. 1 (and also Refs. 15–18) is ~20 MPa, which means $(\sigma_y\text{-}\sigma_f)$ is ~10 MPa if the shear band is indeed cold in the $d=1$ mm sample (this will be justified by the full solution to Eq. (6) later, in a self-consistent manner). We will then use this $(\sigma_y\text{-}\sigma_f)$ and the other properties of this BMG (Fig. 3 caption), to solve Eq. (6) numerically (now with the T effect considered). The output of Eq. (6) predicts the evolution of the displacement x, the sliding speed v, and the temperature T inside the shear band, all as a function of the time elapsed during shear-band sliding. The results are plotted in Fig. 3 and also listed in Table I. For $d=1.0$, 1.5, and 2.0 mm, the sliding clearly goes through an acceleration-deceleration-stop cycle [see the sliding speed plotted in Fig. 3(b)]. When the shear band stops, the predicted shear-step size (Δx) compares very well with the range observed in experiments for these different-sized samples [Fig. 3(a)], adequately explaining the observed scaling of the step size with d (and the step size reported by others for similar sample sizes[15,16]). The time elapsed in this sliding event (a few ms, Fig. 3) agrees with experimental measurements within an order of magnitude.[10–12,15,16] The predicted shear band sliding speed [on the order of 1 mm/s, Fig. 3(b)] is also consistent with a recent estimate (2 mm/s) based on experimental measurements of the time interval and the corresponding strain release in a serration.[11] As for the T rise, Fig. 3(c) predicts only minor increase [well below T_g (Refs. 10 and 11)]. In these smaller samples the shear band is thus indeed *cold*. Its sliding is stable, exhibiting the stop-and-go cycles. This justifies the use of the observed stress drop in Fig. 1 as $2(\sigma_y\text{-}\sigma_f)$, as discussed earlier for the cold-band assumption. As expected for the stick slip, the stress drop (~20 MPa) is observed to be almost constant for this BMG in various experiments.[15–18]

Figure 3 and Table I also predict that for the larger samples with $d=3.0$ and 4.0 mm of the same BMG, the shear displacement (step size) diverges (no stop) and the T in shear band would exceed T_g. Stable serration would then not be possible. Indeed, our $d=3.0$ and 4.0 mm samples showed runaway failure after yielding and the surface sheared apart is overwhelmingly dominated by the familiar vein-like pattern,[18] as opposed to that in Fig. 1(b) for cold sliding. The origin of the catastrophic instability is the rising T. In these larger samples, the shear band accelerates continuously [Fig. 3(a)] and inevitably turns into a hot one [Fig. 3(c)] during a single sliding event.

In addition to this specific quantitative case, Eq. (6) also predicts the general trend for BMGs. Whether or not the serration (or cold shear band) is possible is primarily determined by the competition between the $\frac{Ex}{L(1+S)}$ term and the $\frac{AE^2\varepsilon_y \sin\theta}{2\rho c_p T_g\sqrt{\pi\alpha}}\int_0^t x'(t-\tau)\frac{d\tau}{\sqrt{\tau}}$ term, as the former term reduces the internal driving stress while the latter one reduces the resistance in the flowing shear band. Depending on which of the two is dominant, the *net* driving stress (the entire left side of Eq. (6)) is either positive (accelerating) or negative (decelerating). In the weighting factors, $\frac{E}{L(1+S)}$ and $\frac{AE^2\varepsilon_y \sin\theta}{2\rho c_p T_g\sqrt{\pi\alpha}}$, the parameters are mostly material properties except for $L(1+S)$. For a specific BMG material, when $L(1+S)$ is larger than a critical value of material property, λ_{crit}, the reduction in the internal stress due to elastic unloading is inadequate to compensate for the reduction in resistance due to the T rise. The net driving stress is then always positive and the sliding would continue on without ever stopping, feeding more and more energy into the shear band and continuously raising the T, which in turn drives the shear out of control. This is thus a catastrophic shear band.

Therefore, λ_{crit} can be used to evaluate the intrinsic ability of the material to sustain stable plastic deformation and it may have some connections with the toughness (e.g., K_{IC}). The λ_{crit} has a unit of length and it can be intuitively per-

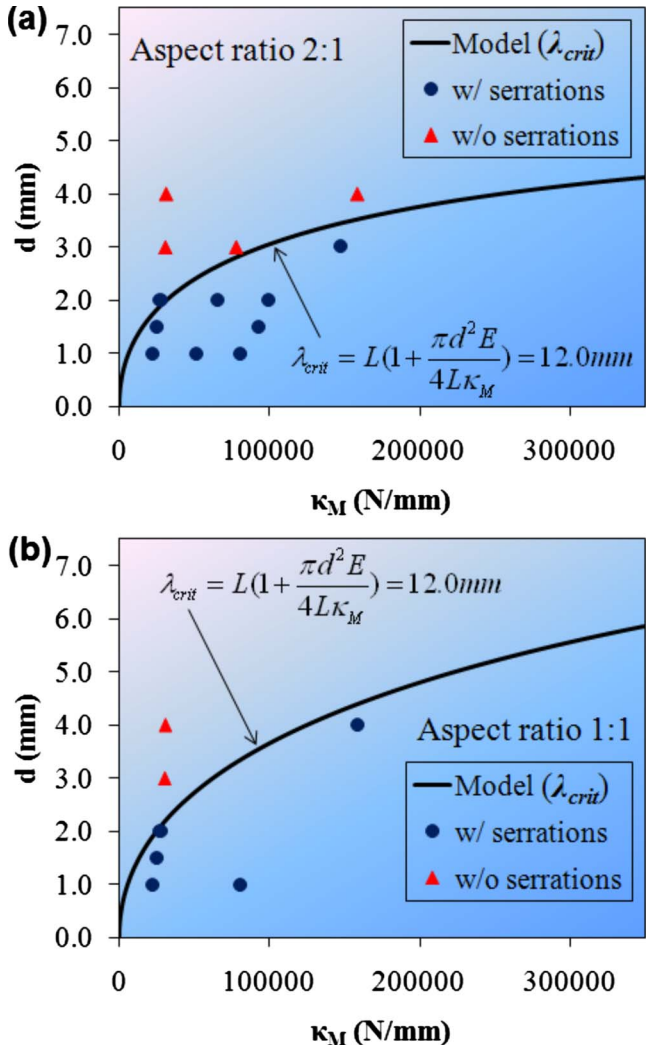

FIG. 4. (Color online) The predicted functional form of λ_{crit} separates very well the two shear-band regimes (stick slip versus runaway instability) observed in experiments (Ref. 17). Here, d denotes the sample diameter and κ_M denotes the machine stiffness. Two different sample-aspect ratios exhibit consistent λ_{crit}, indicating that λ_{crit} is a material property related to intrinsic plasticity.

ceived as the upper limit of sample size above which the sliding of a single band in the sample is intrinsically unstable. In Fig. 4, we have plotted a boundary line in the functional form of $L(1+S)=\lambda_{crit}=$constant, which well separates the available experimental data for different sample d, aspect ratio, and κ_M.[17] One can see that cold shear banding with slow stop-and-go growth of the shear offset is more likely in small-scale samples; an extreme case was in fact observed before in *in situ* transmission electron microscopy tests of submicron-sized BMG pillars.[31,32] In the videos recorded,[31] the shear band shows an instantaneous speed of a few hundred nanometers per second, orders of magnitude smaller than that in the conventional bulk samples (including those in Table I). The shear band there exhibits clear stick-slip behavior. Our analysis presented in this paper thus offers another explanation of the observed sample-size effects on the plastic-deformation behavior of metallic glasses.

Finally, we briefly address a few issues related to the present modeling work. The effective inertia M in Eq. (2) is not a measurable quantity although we have provided an estimated range for it. While there might be quantitative uncertainties, its qualitative implication is clear: In a realistic experiment, the machine and its response must be considered during shear-band sliding. Although the sliding time in our case changed by a factor of 2 when M changes from 10 to 100 kg, the order of magnitude and the major conclusions are not affected by the exact value of M, provided that it represents the whole MSS, and falls in the reasonable range (e.g., $M=50$ kg in Fig. 3).

Figures 1(a) and 1(c) show a small decrease in stress and increase in stress drop at larger plastic strains. Presumably this is partly because the increasing shear off gradually influences the loading geometry and stress field. Such effects are beyond the scope of the current model. In fact, the present work addresses whether flow serrations can be observed or the sample fails quickly after yielding. Experimentally, however, even samples showing flow serration at the beginning of the stress-strain curve may finally fail on catastrophe, at large plastic strains. The instability in this case is likely to be assisted by the distorted loading geometry, which may lead to the formation of microcavitations and microcrack, etc. These are additional extrinsic factors introduced during deformation; the intrinsic material property (e.g., the initial σ_f at T_R) in the shear band, however, is not expected to change significantly with increasing strain.

In experiments, plastic strains may also arise from more than one shear band, and the serrations observed in the stress-strain curve may thus correspond to the initiation of multiple shear bands, which is different from the scenario discussed in this paper. However, if the major shear band is catastrophic (assuming not arrested by confinement or nanoscale entities such as crystals), it would leave no time for other shear bands to develop. Therefore, the cold shear banding and the stop-and-go stick slip should be important for giving other shear bands a chance to contribute to the plastic strains.

We are aware that there have been other papers (e.g., Refs. 8 and 10–13) that model the temperature in shear band, where experimentally observed shear step size and sliding time are used as *input* to estimate the sliding speed and the final temperature in the shear band. The equation used is based on the assumption of constant heat flux for the whole process.[30] Different from previous models, here we are modeling the stick-slip cycle and we do so using minimum experimental input (mostly sample/machine properties). The offset step size, sliding time, sliding speed, and temperature are all *output* results of the model. These results can then be compared with experimental measurements, such as those in Fig. 1 and in Ref. 11. In addition, our model also predicts the dependence of these output results on sample size and machine stiffness, and explains the bifurcated shear-banding behaviors (stick slip versus catastrophe). The underlying competition between the rates of stress release and temperature rise is discussed. The heat flux in our model is not assumed to be constant but scales with the instantaneous sliding speed so that the self-propelling nature of the shear-band instability is better captured and described.

IV. CONCLUSIONS

In summary, in a displacement-controlled compression test of a BMG, the dominant shear band can slide in a stick-slip manner, giving rise to controlled and sustained plastic strain. Our analysis predicts an acceleration-deceleration cycle that explains the stop-and-go behavior observed in experiments. The temperature rise in such shear bands are predicted to be very small, quantitatively illustrating that such shear bands can be cold. We have explained why the shear step size of the serration is observed to scale with $L(1+S)$, demonstrating that there should be sample-size effects and machine-stiffness effects (such as those in Figs. 1 and 4). For example, for a given shear-banding displacement, a smaller sample experiences a larger strain and hence a larger elastic unloading of the stress to cause a more pronounced deceleration of the shear band. We also calculated the speed at which the shear offset grows, which compares favorably with experimental measurements (e.g., Refs. 10 and 11). In addition, for a specific BMG there is a critical value λ_{crit} for $L(1+S)$, above which the shear band becomes hot instead, and is hence unstoppable. The use of the S index alone[17] as the indicator is inadequate in this regard. For example, with d fixed, a larger L would lead to a smaller S, which means stable serration is more likely (i.e., S is less likely to exceed its critical value for the given BMG). This is inconsistent with experimental observations. The new instability index $L(1+S)$ resolves this paradox and is expected to be a more appropriate indicator to predict the stability trends (Fig. 4). This λ_{crit}, which is a material property, can be used to evaluate the intrinsic plasticity of the BMG. Cold shear banding provides an explanation to the "large plasticity" observed in some BMGs, especially in small (on the order of 1 mm) samples and in submicron pillars.[31,32] In these cases, experimentally it is indeed observed that the shear band exhibits the stop-and-go behavior, low speed of the shear offset growth, and striations on the sheared surfaces.[15,16,18,31] Of course, multiple shear bands do often come into play in BMGs that can accommodate large plastic strains. However, as the hot shear bands tend to be catastrophic, the controlled and serrated sliding of the major shear band is also an important condition for multiple shear bands to have the opportunity to contribute to the plastic deformation. As such, the discussion here regarding the regime of cold shear banding should have impact on the understanding of shear-band behavior in BMGs.

ACKNOWLEDGMENT

This work was supported by U.S. DOE-BES, Division of Materials Sciences and Engineering, under Contract No. DE-FG02-09ER46056.

*mseliy@nus.edu.sg
†ema@jhu.edu

[1] A. L. Greer and E. Ma, MRS Bull. **32**, 611 (2007).
[2] C. A. Schuh, T. C. Hufnagel, and U. Ramamurty, Acta Mater. **55**, 4067 (2007).
[3] A. R. Yavari, J. J. Lewandowski, and J. Eckert, MRS Bull. **32**, 635 (2007).
[4] M. W. Chen, Annu. Rev. Mater. Res. **38**, 445 (2008).
[5] D. C. Hofmann, J.-Y. Suh, A. Wiest, G. Duan, M.-L. Lind, M. D. Demetriou, and W. L. Johnson, Nature (London) **451**, 1085 (2008).
[6] Y. H. Liu, G. Wang, R. J. Wang, D. Q. Zhao, M. X. Pan, and W. H. Wang, Science **315**, 1385 (2007).
[7] J. Das, M. B. Tang, K. B. Kim, R. Theissmann, F. Baier, W. H. Wang, and J. Eckert, Phys. Rev. Lett. **94**, 205501 (2005).
[8] J. J. Lewandowski and A. L. Greer, Nature Mater. **5**, 15 (2006).
[9] T. C. Hufnagel, T. Jiao, Y. Li, L. Q. Xing, and K. T. Ramesh, J. Mater. Res. **17**, 1441 (2002).
[10] W. J. Wright, R. B. Schwarz, and W. D. Nix, Mater. Sci. Eng., A **319-321**, 229 (2001).
[11] W. J. Wright, M. W. Samale, T. C. Hufnagel, M. M. LeBlanc, and J. N. Florando, Acta Mater. **57**, 4639 (2009).
[12] F. H. Dalla Torre, A. Dubach, J. Schällibaum, and J. F. Löffler, Acta Mater. **56**, 4635 (2008).
[13] K. Georgarakis, M. Aljerf, Y. Li, A. LeMoulec, F. Charlot, A. R. Yavari, K. Chornokhvostenko, E. Tabachnikova, G. A. Evangelakis, D. B. Miracle, A. L. Greer, and T. Zhang, Appl. Phys. Lett. **93**, 031907 (2008).
[14] Y. Zhang, N. Stelmashenko, Z. Barber, J. J. Lewandowski, and A. L. Greer, J. Mater. Res. **22**, 419 (2007).
[15] S. X. Song, H. Bei, J. Wadsworth, and T. G. Nieh, Intermetallics **16**, 813 (2008).
[16] S. X. Song and T. G. Nieh, Intermetallics **17**, 762 (2009).
[17] Z. Han, W. F. Wu, Y. Li, Y. J. Wei, and H. J. Gao, Acta Mater. **57**, 1367 (2009).
[18] Z. Han and Y. Li, J. Mater. Res. (to be published).
[19] T. Murata, T. Masumoto, and M. Sakai, in *Proceedings of 3rd International Conference on Rapidly Quenched Metals*, edited by B. Candor (The Metals Society, London, 1978), Vol. 2, p. 401.
[20] B. Bhushan, *Introduction to Tribology* (Wiley, New York, 2002), p. 207.
[21] F. Shimizu, S. Ogata, and J. Li, Acta Mater. **54**, 4293 (2006).
[22] Y. Q. Cheng, A. J. Cao, H. W. Sheng, and E. Ma, Acta Mater. **56**, 5263 (2008).
[23] W. L. Johnson, J. Lu, and M. D. Demetriou, Intermetallics **10**, 1039 (2002).
[24] W. L. Johnson, M. D. Demetriou, J. S. Harmon, M. L. Lind, and K. Samwer, MRS Bull. **32**, 644 (2007).
[25] H. Li, C. Fan, H. Choo, and P. K. Liaw, Mater. Trans. **48**, 1752 (2007).
[26] D. H. Xu, B. Lohwongwatana, G. Duan, and W. L. Johnson, Acta Mater. **52**, 2621 (2004).
[27] C. E. Packard and C. A. Schuh, Acta Mater. **55**, 5348 (2007).
[28] M. D. Demetriou, W. L. Johnson, and K. Samwer, Appl. Phys. Lett. **94**, 191905 (2009).
[29] W. L. Johnson and K. Samwer, Phys. Rev. Lett. **95**, 195501 (2005).
[30] H. S. Carslaw and J. C. Jaeger, *Conduction of Heat in Solids* (Oxford University Press, Oxford, 1948), p. 76.
[31] Z. W. Shan, J. Li, Y. Q. Cheng, A. M. Minor, S. A. Syed Asif, O. L. Warren, and E. Ma, Phys. Rev. B **77**, 155419 (2008).
[32] H. Guo, P. F. Yan, Y. B. Wang, J. Tan, Z. F. Zhang, M. L. Sui, and E. Ma, Nature Mater. **6**, 735 (2007).